Particle acceleration in 3D single current sheets formed in the solar corona and heliosphere: PIC approach

Valentina V. Zharkova [1]**& Taras Siversky**[2]

[1] Department of Mathematics and Information Sciences, Northumbria University, Newcastle upon Tyne, NE2 1XE, UK

[2] Department of Radiophysics, T.Shevchenko National University of Kyiv, 8 Glushkov prosp., Kyiv, 03022, Ukraine

E-mail: valentina.zharkova@northumria.ac.uk

Abstract. Acceleration of protons and electrons in a reconnecting current sheet (RCS) is investigated with the test particle and particle-in-cell (PIC) approaches in a 3D magnetic topology. PIC simulations confirm a spatial separation of electrons and protons with respect to the midplane depending on the guiding field. Simulation reveals that the separation occurs in magnetic topologies with strong guiding fields and lasts as long as the particles are kept dragged into a current sheet. This separation produces a polarisation electric field induced by the plasma feedback to a presence of accelerated particles, which shape can change from symmetric towards the midplane (for weak guiding field) to fully asymmetric (for strong guiding field). Particles are found accelerated at a midplane **of any current sheets present in the heliosphere** to the energies up to hundred keV for electrons and hundred MeV for protons. The maximum energy gained by particles during their motion inside the current sheet is defined by its magnetic field topology **(the ratio of magnetic field components), the side and location from the X-nullpoint, where the particles enter** a current sheet. **In strong magnetic fields of the solar corona with weaker guiding fields, electrons are found circulating about the midplane to large distances where proton are getting accelerated, creating about the current sheet midplane clouds** of high energy electrons, which can be the source of hard X-ray emission in the coronal sources of flares. **These electrons are ejected into the same footpoint as protons after the latter reach the energy sufficicent to break from a current sheet.** In a weaker magnetic field of the heliosphere the bounced electrons with lower energies cannot reach the midplane turning instead at some distance D before the current sheet midplane by 180 degrees from their initial motion. Also the beams of accelerated transit and bounced particles are found to generate turbulent electric fields in a form of Langmuir waves (electrons) or ion-acoustic waves (protons).

1. Introduction

In the present paper we investigate particle acceleration by a drifted (reconnection) electric field generated by a reconnecting current sheet (RCS). The first analytical study of this acceleration mechanism was proposed by Speiser[1] who found that the particles can be accelerated to rather high energies after they enter the configuration with reconnecting magnetic field lines forming an RCS and a perpendicular (drifted) electric field. This theory was extended by Litvinenko

and Somov [2, 3] who found that the guiding magnetic field can significantly increase the energy gains by accelerated particles.

Simulation of particle trajectories by using test particle approach in a 3D RCS was carried for a constant reconnection electric field [4] or for a variable electric field enhanced near the X-nullpoint due to anomalous resistivity [6]. Zharkova and Gordovskyy [4] showed that the trajectories of particles with the opposite charges (electrons or protons) can be either fully symmetric or strongly asymmetric towards the midplane of the RCS depending on the ratio between the magnetic field components.

As a result, some fraction of the released magnetic energy is transformed into kinetic energy of accelerated particles. The energy spectra of these particles also depend on a magnetic field topology, electric field strength and the dependence of transverse magnetic field on a distance from the X-nullpoint. **Particles are accelerated at a current sheet midplane (X=0)[4, 5], the longer they gyrate about the Y and Z components the higher energy they gain from a reconnection electric field E_y (see Fig.1). The particles can break from a current sheet only after they gain the critical energy defined by a given magnetic field topology[7].** Accelerated particles gain energies up to 100 keV for the electrons and up to 100 MeV for the protons [6, 8, 9]. Spectral indices of energy spectra gained at acceleration vary from 2 for electrons and 1.5 for protons if the transverse magnetic field increases with the distance linearly. The spectral indices for both electrons and protons become much higher if the transverse magnetic field $B_x(z)$ increases exponentially with a distance z from the X-nullpoint towards its full length a (e.g $B_x(z) = B_0 \cdot (\frac{z}{a})^n$ having index n>1 near the ratio z/a) [5, 9].

More realistic approach considering plasma feedback to accelerated particles in current sheet in the solar corona is achieved with PIC simulation for reduced proton-to-mass ratios allowing to reproduce electro-magnetic fields generated by accelerated particles in solar flares [10, 11, 12]. These studies reproduced well magnetic reconnection rates [10] and some key features of accelerated particles; power law energy spectrum and energy gains up to 100 keV.

Recent study of particle acceleration during a magnetic reconnection with PIC approach in a 3D single current sheet by Siversky and Zharkova [12] for conditions of the solar corona and by Zharkova and Khabarova [13] for conditions of the heliospheric current sheet have shown that magnetic field topology defines the energy gains, pitch angle and density distributions of electrons and protons after their passage through the current sheet. Of course, the findings are derived only for a single current sheet while Drake et al [14] have shown that during a magnetic reconnection a current sheet can be broken by tearing instability into a few magnetic islands where particle acceleration scenario can change.

However, for the current study we continue to investigate particle passage through and gaining energy in a single current sheet and compare particle characteristics in the current sheets with stronger magnetic field and denser plasma (close to the solar corona) and in the current sheets with low density and low magnetic field magnitudes relevant to the heliosphere.

2. Description of the model

In this paper we apply the PIC approach for the simulation of particle acceleration in a 3D reconnecting current sheet with a simple 3D magnetic field topology. We assume that the current sheet plasma has typical density of either the solar corona or the heliosphere, which sustain the equilibrium with the background magnetic field. However, in order to avoid the problem with the small Debye length in PIC approach, only a small fraction of the plasma particles (with density of $10^{10} m^3$) is included in the PIC simulation for the solar corona and $1 - 10^6\ m^3$ in the heliosphere. Electric and magnetic fields generated by the accelerated particles in the PIC approach are used in the TP approach to investigate particle trajectories and densities.

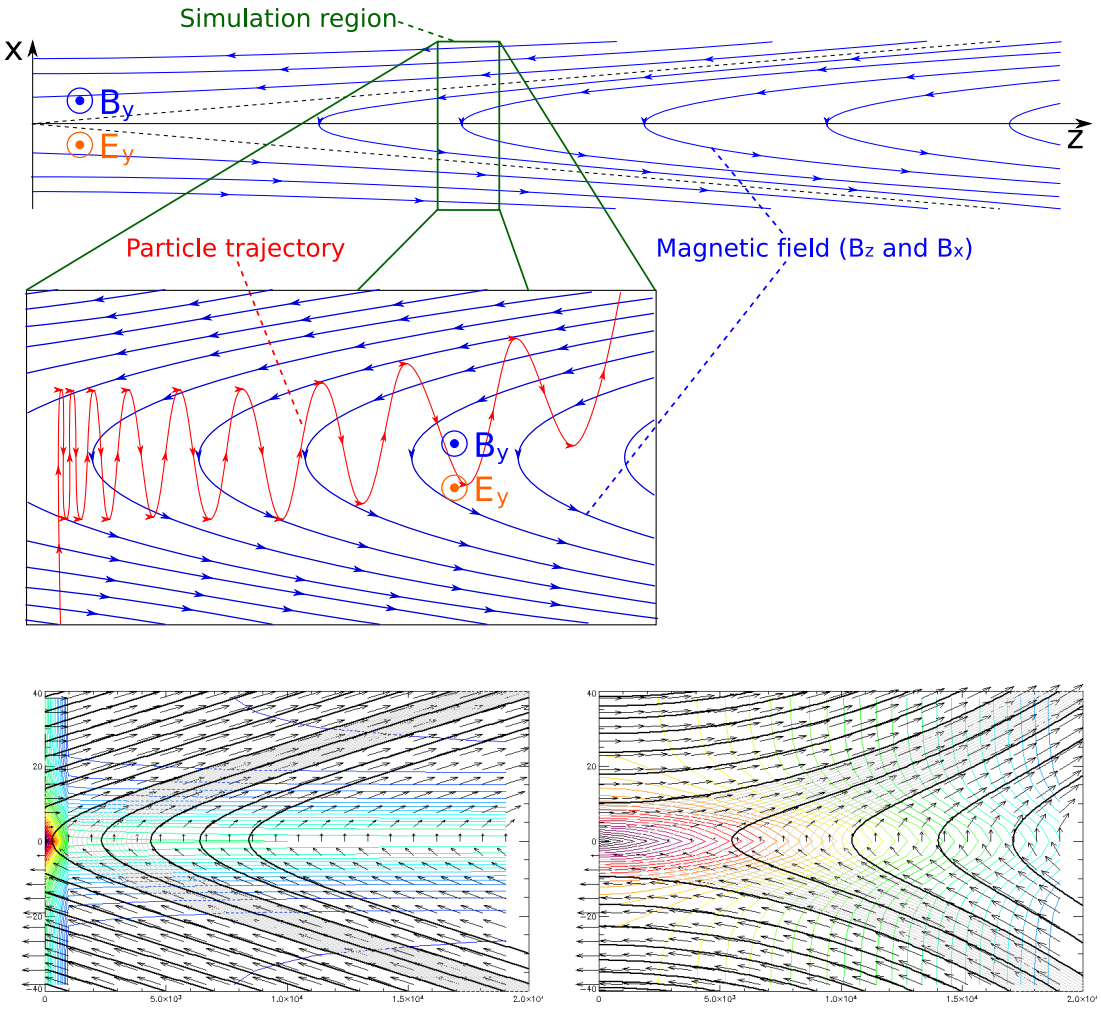

Figure 1. Model of 3D current sheet used in the PIC simulations for the sliding region shown (the top plot). Current sheet topologies for different values of the parameter α describng the variations of transverse magnetic field $B_x(z) = B_{x0}(\frac{z}{L_z})^{\alpha}$: $\alpha = 0.5$ (the bottom left plot), 1.5 (the bottom right plot).

2.1. Magnetic field topology

Since the acceleration time electrons or protons is much shorter than the time of a reconnecting magnetic field variation as shown by Priest and Forbes [15], one can assume the background magnetic field to be stationary. Also, from the TP simulations one found that travel distances of accelerating particles along the RCS are of the order of 10 km at most (for the protons) [9] and this length is much shorter than the length scale of magnetic field variations along the current sheet. In addition, we assume that the magnetic field variations across the current sheet have much shorter length scale than along the current sheet, i.e. $L_x \ll L_z$, L_y.

The simulation domain is a small part of the RCS (see Fig. 1 from [12]), but still large enough to contain the full trajectories of accelerated particles if the periodic boundary conditions are used. Previously, it was shown[9] that electrons normally travel the distances of about a few hundred meters for the coronal conditions (with proton gyroradius is about 1 m) while protons travel a few thousand meters before they gain energy sufficient to get ejected from a current sheet.

The main component B_z depends on x as follows: $B_z(x) = -B_{z0}\tanh\left(\frac{x}{L_x}\right)$. Similar to Zharkova and Gordovskyy [5], **it is assumed that the B_x component varies** inside the simulation domain with z as follows, i.e. $B_x(z) = -B_{x0}(\frac{z}{L_z})^{\alpha}$ where α >1. In Fig. 1 (bottom two plots) the views of magnetic field topologies in reconnecting current sheet are presented for two magnitudes of the spectral parameter α. The guiding (out-of-plane) magnetic field B_y is maximal in the midplane and vanishes outside the RCS: $B_y(x) = B_{y0}\mathrm{sech}\left(\frac{x}{L_x}\right)$. We show below that this parameter α defines spectral indices of energy spectra for both kinds of particles: electrons and protons, depending in the ratio between magnetic field components.

Contrary to the TP simulations, in the PIC simulations the accelerated particles are considered to generate their own electric and magnetic fields following the plasma feedback according to the Maxwell's equations, which is self-consistently taken into account as described by Siversky and Zharkova [12].

2.2. Reconnection electric field

In order to provide the inflow of plasma in the simulation domain we set up a background electric field, as the one drifted in by a magnetic diffusion process with velocity V_{in} as shown by [15]: $E_{y0} = V_{in} \times B_{z0} + \frac{1}{\sigma\mu}\frac{\partial B_z}{\partial x}$, where V_{in} is the inflow velocity, σ is the ambient plasma conductivity, μ is magnetic permeability. On the boundaries of an RCS we ignore a gradient of the magnetic component B_z over x-coordinate by putting the second term to zero.

Simulations are carried out for the following current sheet parameters: the main component of the magnetic field $B_{z0} = 10^{-3}$ T , the current sheet half-thickness $L_x = 1$ m, the drifted electric field $E_{y0} = 250$ V/m and the guiding, B_{y0}, and transverse, B_{x0}, components of the magnetic field are selected to range from $(0.1 - 10) \times 10^{-4}$ T, in order to cover acceleration at the various parts of RCS in the solar corona.

3. Results

3.1. Polarization electric field induced by accelerated particles

The PIC simulations have shown that the magnetic field $\tilde{\mathbf{B}}$ induced by the plasma feedback to a sepration of accelerated particles in the ambient plasma is much smaller than the background $\mathbf{B_z}$. On the other hand, the induced electric field $\tilde{\mathbf{E}}_\mathbf{x}$, called a polarization electric field, induced by the separation of electrons from protons is much larger than the reconnection (drifted) field E_y [9, 12].

In this subsection we consider this polarization electric field $\tilde{E}_x$, which is directed across the current sheet along X-axis and plotted in Fig. 2 as a function of x averaged over the z coordinate for various magnetic field parameters of B_{x0} and B_{y0}. The appearance of polarization electric field leads to a local non-neutrality of the plasma, which becomes stronger if the transverse magnetic field B_{x0} decreases or the guiding magnetic field B_{y0} increases.

The polarisation electric field defines the motion of charged particles in the vicinity of a current sheet, which can be captured from the ion velocity profiles by in-situ observations with the spacecrafts passing through the heliospheric current sheet (or crossing the sector boundary)[13].

3.2. Proton trajectories

In order to reconstruct the particle trajectories, we use a TP approach, where the induced polarisation electric field $\tilde{E}_x$ obtained from PIC is added to the background electro-magnetic configuration described above. The trajectories of the two protons in the x-V_z phase plane entering current sheet from the opposite directions are shown in Fig. 3 for magnetic field topology forming a polarisation field from Fig. 2 (the left plot).

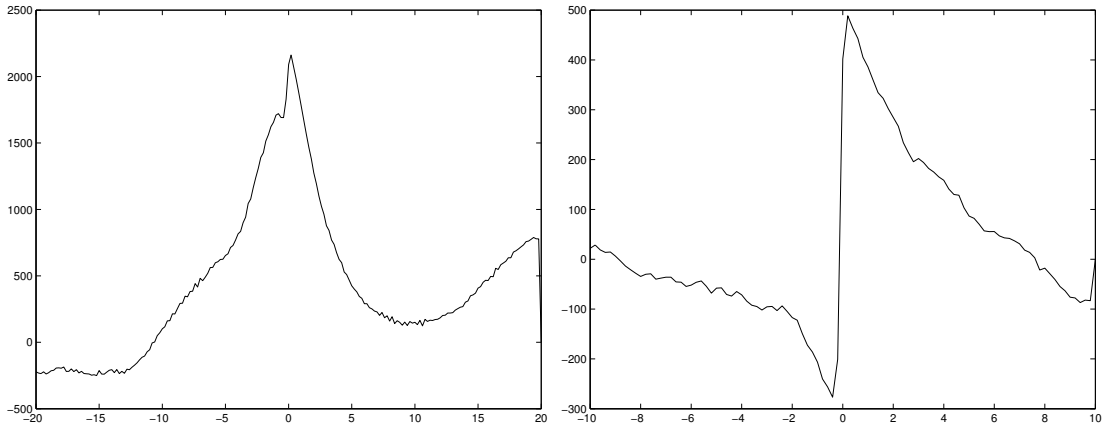

Figure 2. Polarisation electric field $\tilde{E}_x$ **(Y-axis, V/m)** induced by accelerated particles as derived from the PIC simulations in the corona for $B_{z0} = 10^{-3}$ T and the following values of other components: $B_{x0} = 10^{-4}$ T and $B_{y0} = 10^{-6}$ T (left plot) and $B_{x0} = 10^{-5}$ T and $B_{y0} = 2 \times 10^{-3}$ T (right plot). **X-axis represents distances from a current sheet midplane (X=0). Note that the reconnection electric field is equal to 100 V/m and a current sheet width is 2 m (1 m to each side).**

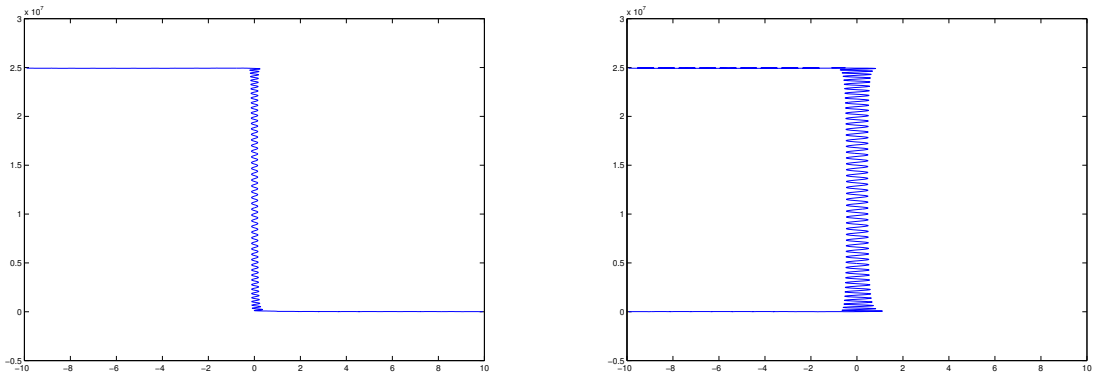

Figure 3. Trajectories and velocities (Y-axis, m/s) of the transit (left plot) and bounced (right plot) protons entering a current sheet from the 3D PIC simulation for the coronal magnetic field topologies: $B_{z0} = 10^{-3}$ T, $B_{x0} = 10^{-4}$ T and $B_{y0} = 10^{-4}$ T. **The X axis presents a distance (in gyroradius of protons, 1 m in the coronal field) from the current sheet midplane (X=0).**

First, we note that the "bounced" protons have wider orbits of their gyration about the midplane than the "transit" ones. Second, the presence of polarisation electric field makes very peculiar velocity profiles of protons and ions which follow the profile of this polarisation field.

These trajectories are rather similar to those obtained in the TP simulations without $\tilde{E}_x$ with the "bounced" proton during the acceleration phase has a wider orbit while the "transit" proton has a narrower one producing energy distributions with two peaks discussed below.

3.3. Electron trajectories and formation of electron clouds

Electrons entering from the $x < 0$ semispace have a dynamics similar to those of the "transit" protons, e.g. the electrons drift towards the midplane, become accelerated and ejected to the

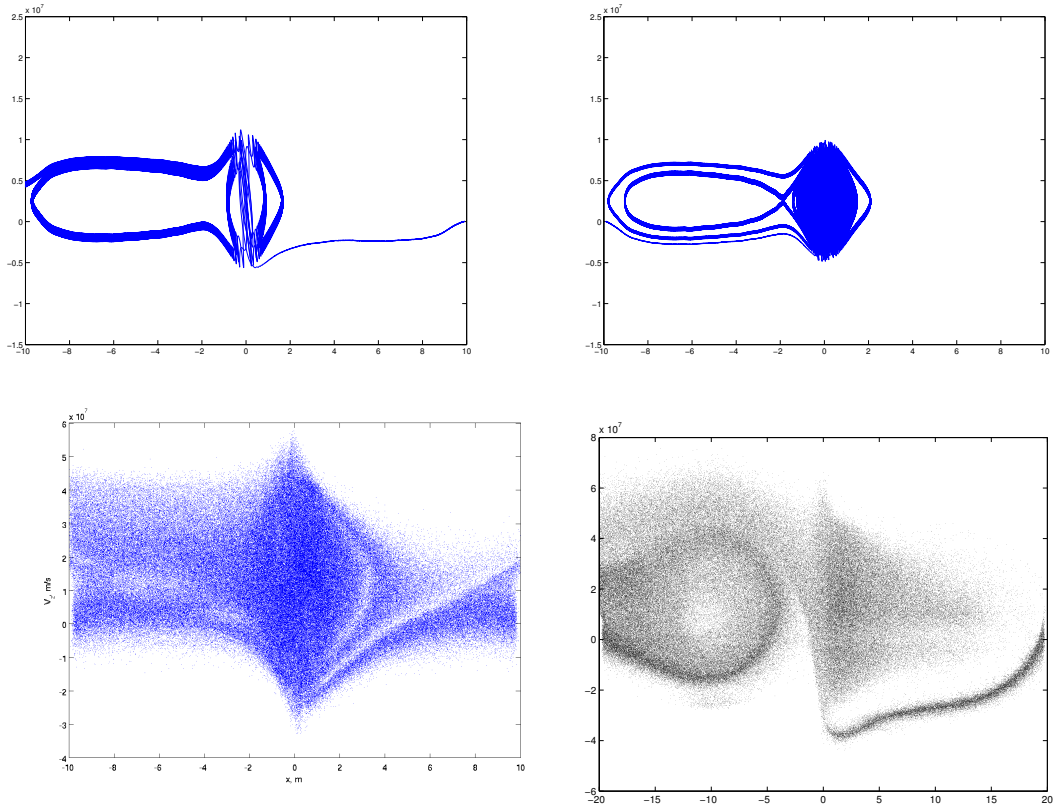

Figure 4. Electron velocity distribution **(Y-axis, m/s)** showing formation of the clouds from transit electrons about the midplane and from bounced electrons far away from the midplane as deduced from the 3D PIC simulation. **Test particle trajectories of transit electron (top left plot) and bounced electron (top right plot) during their circulation about the midplane for the coronal magnetic field:** $B_{z0} = 10^{-3}$ **T,** $B_{x0} = 10^{-4}$ **T and** $B_{y0} = 10^{-4}$ **T. PIC simulations of electron motion and formation of clouds from the transit (bottom left plot) and bounced (bottom right plot) electrons calculated for the magnetic field topology:** $B_{z0} = 10^{-3}$ **T,** $B_{x0} = 10^{-4}$ **T and** $B_{y0} = 10^{-5}$ **T.**

$x > 0$ semispace. However, the polarization field $\tilde{E}_x(x)$, which extends beyond the current sheet and has a component parallel to the magnetic field B_z, decelerates the ejected electrons. For chosen magnitudes of B_x and B_y, the majority of electrons are unable to escape away from the RCS, instead they are dragged back towards the current sheet and become undistinguishable from the other electrons entered from the $x > 0$ semispace.

The electrons entering from the positive x side which are "bounced" from RCS in the absence of $\tilde{E}_x$, are able to reach its midplane if polarization field is present. In the vicinity of the midplane, the electrons become unmagnetized and oscillate with the gyrofrequency determined by B_y until they gain sufficient energy to break from the magnetic field. Although, if the electron initial velocity is small, it can be quasi-trapped inside the RCS (Fig. 4, top plots).

Such electrons are accelerated at the midplane, ejected from it, then decelerated outside the RCS and returned back to it because of the polarization electric field appearing due to the protons still being accelerated in the RCS midplane. This cycle is repeated for many times, forming the electron clouds around the current sheet (Fig. 4, top plots for TP, bottom plots for PIC) which can be observed as a coronal source in solar flares. These electron clouds exist until the protons gyrate about the midplane and gain sufficient energy to leave the current sheet.

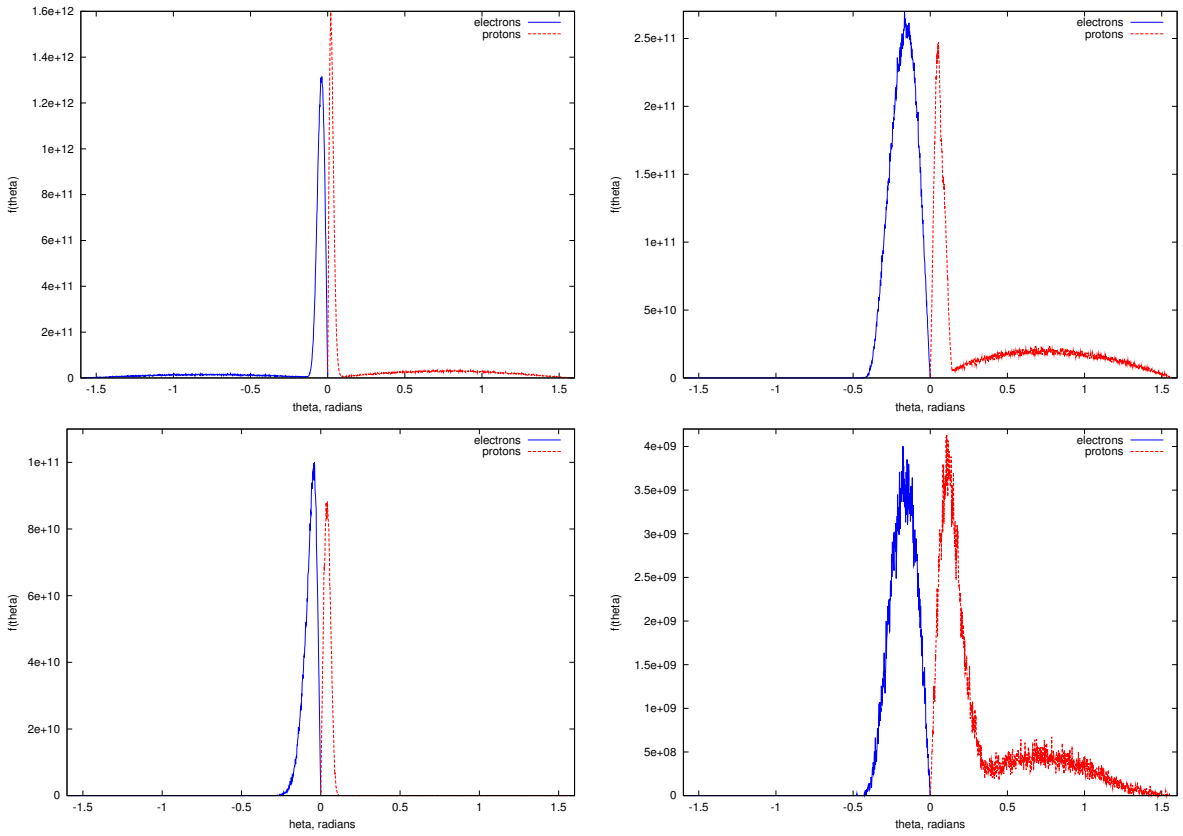

Figure 5. Pitch angles (in radians) of electrons (blue plots) and protons (red plots) calculated for weak guiding field ($B_y/B_z < 10^{-4}$) with the symmetric polarisation electric field (left column) and strong guiding field ($B_y/B_z = 0.1$ (top plot) and $B_y/B_z = 2$ (bottom plot)) with the strongly asymmetric polarisation electric field (right column).

Since a magnitude of the polarisation field $\tilde{E}_x(x)$ is smaller in the current model at $x < 0$ than at $x > 0$ (see Fig. 2, the bottom left plot), for electrons it is easier to escape to the $x < 0$ semispace, where the protons are ejected.

3.4. Energy spectra of electrons and protons

The spectral indices of energy spectra for electrons and protons accelerated by the drifted electric field are found to be strongly dependent on the magnetic field topology [9, 5]. For the accepted variations of B_x being proportional to $(\frac{z}{L_z}))^{\alpha}$ and for the assumed linear increase of the density with z as $(\frac{z}{L_z}))^{\lambda}$ in a vicinity of the X-nullpoint the spectral indices of particles are defined as follows[9] :

For electrons in RCS with weak guiding field, $B_x >> B_y$:

$$\gamma = 1 + \frac{2+\lambda}{2\alpha} \tag{1}$$

For electrons in RCS with strong guiding field, B_y:

$$\gamma = \frac{1}{2} + \frac{1+\lambda}{2\alpha} \tag{2}$$

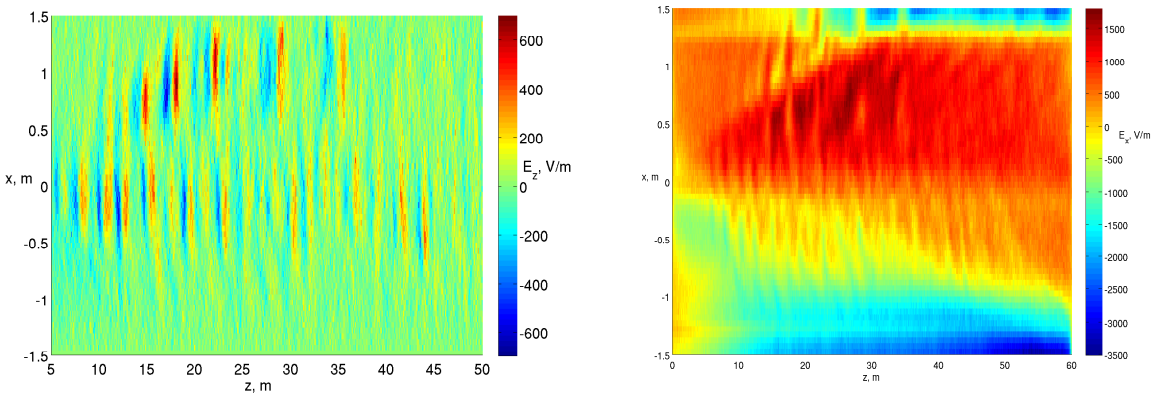

Figure 6. Turbulent electric field along Z axis (the left plot) and X axis (the right plot) induced by the transit and bounced electron beams. Turbulent electric field $\tilde{E}_z$ (the left plot) and $\tilde{E}_x$ (the right plot) induced by particles in PIC simulation ($B_{z0} = 10^{-3}$ T, $B_{y0} = 10^{-4}$ T, $B_{x0} = 4 \cdot 10^{-5}$ T, $E_{y0} = 250$ V/m, $m_p/m_e = 10$, $n = 10^{12}$ m^{-3}.

For protons in RCS with any magnetic field:

$$\gamma = 1 + \frac{1+\lambda}{2\alpha} \tag{3}$$

It can be spotted that for strong guiding fields the spectral indices of electrons and protons become rather close, while for a weaker guiding field the spectral indices of electrons are higher by unit or so than those of protons.

3.5. Pitch-angle distributions of particles at ejection from a current sheet

There are interesting pitch angle distributions of accelerated particles with respect to B_z after their ejection from the simulation region shown in Fig. 5. Pitch angle dispersion of accelerated particles increases the case of a strong guiding field (Fig. 5, the right column of plots) while being rather narrow **(focused along the component B_z) (Fig. 5, the left column of plots).**

At the same time, the decrease of the transverse magnetic field B_x (Fig. 5, the bottom row plots) leads to wider pitch angle distributions compared to a higher B_x (located far away from the X-nullpoint) (Fig. 5, the top row plots).

3.6. Turbulence generated by bounced and transit beams

As it can be seen from the PIC simulation shown in Fig. 6, we detect formation of turbulence with the induced electric field components, $\tilde{E}_z$ and $\tilde{E}_x$ being structured with a characteristic length scale of about $\lambda_{wave} \approx 2m$ for the conditions of the solar corona or $2 \times 10^5 m$ for the heliosphere at 1 AU. This structure propagates in time in the positive direction of the z axis.

The speed of this propagation is about $V_{wave} \approx 1.3 \cdot 10^7 m/s$, which makes the temporal period of oscillations about $T_{wave} \approx 1.5 \cdot 10^{-7}$ s. Since the plasma frequency in the corona for $n = 10^{12}$ m^{-3} is $9.1 \cdot 10^6$ Hz, the generated wave is the Langmuir wave (see Fig. 6). The same applies to the conditions of the heliosphere. Note also that the oscillating component of the excited wave $\tilde{E}_z$ is parallel to the direction of propagation, which indicates a linear polarisation of Langmuir wave generated.

The plots a V_z distribution function of electrons (see Fig. 7) in the region where the instability occurs (some rectangular region in Fig. 6) indicates that the electrons have the typical unstable

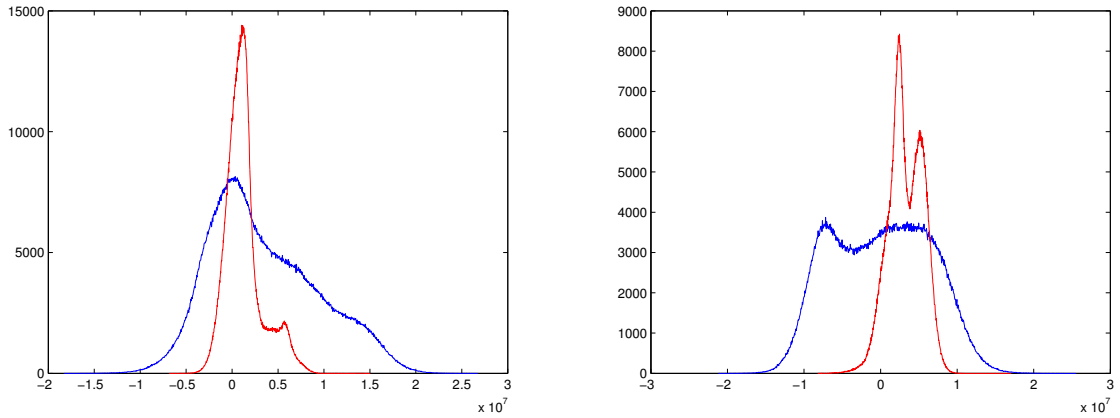

Figure 7. Density distributions (Y axis, arbitrary units) of electrons (blue) and protons (red) versus velocities (X axis, m/s) showing the double maxima defined by the difference in acceleration scenario for transit and bounced by electrons/protons. These distributions lead to the two beam instability and formation of turbulence, examples of which**(formed by the transit and bounced electron beams)** are shown in Fig. 6.

distribution with "bump-in-tail". The range of velocities V_z for which the derivative df/dV_z is positive is from $1.3 \cdot 10^7$ to $2 \cdot 10^7$ m/s, these values correspond to the phase velocity of the Langmuir wave V_{wave} deduced earlier.

The generation of Langmuir waves is not the only possible instability to occur in an RCS but can also lead to excitation of whistler or ion-acoustic waves as was shown by Shay et al [16, 17]. This statement is supported by the distributions of accelerated protons (see Fig. 7, red lines) showing a presence of 'bump-in-tail in the proton distributions.

However, in our current PIC simulations we can only observe the waves with the length scales less than the size of the simulation domain. Also, since the current simulation system is 2D in space (and 3D in velocities), some ion waves, which are essentially 3D cannot be generated in the current model. The investigation of other instabilities, apart from Langmuir waves, can be a scope of the forthcoming study.

4. Conclusions

The PIC simulation has shown that accelerated particles produce a strong polarisation field, $\tilde{E}_x$, caused by the separation of accelerated protons from electrons across the current sheet midplane. This polarisation field is shown to have much higher magnitudes that the reconnection electric fiel that leads to essential modification of the trajectories of electrons, and, to some extent, of protons.

The polarisation electric field can be essentially skewed towards one or another semiplane, with respect to the midplane, where the magnetic field components are weaker, or become strongly asymmetric, if the guiding field is strong and comparible with the main component B_z.

Electric polarisation field affects in different ways the "transit" particles (those which enter from and are ejected to the opposite semispaces towards the midplane) and "bounced" particles (those which enter from and are ejected to the same semispace towards the midplane). First, we note that the "bounced" protons have wider orbits of their gyration about the midplane than the "transit" ones. Second, the presence of polarisation electric field makes very peculiar velocity profiles of protons and ions which follow the profile of this polarisation field.

Moreover, the electrons, which are "bounced" in the TP approach, in the PIC simulations

are dragged by the polarisation field $\tilde{E}_x$ back towards the midplane. Depending on the magnetic field magnitudes, ratio of the component and the ambient plasma density, the bounced electrons can either reach the midplane (in the case of the coronal parameters)[12] or are turned back from a current sheet (in the case of the HCS parameters) [13].

At the same time, the "transit" electrons, which are ejected to the opposite semispace from protons in the TP approach travel from the current sheet to a distance up to 10 (or larger) sizes of RCS thickness and then are dragged back to the RCS by the polarisation field $\tilde{E}_x$. This process results in formation of electron clouds around current sheet midplane, which exist as long as protons are being accelerated on that midplane. As result, in the PIC model with a weaker polarization field the protons are often found ejected along with electrons to the same side from the midplane, contrary to the full separation detected in pure TP simulations.

Electrons and protons gain energy from the current sheets forming power law energy spectra with either the close spectral indices (for magnetic field topologies with strong guiding field) or with electrons spectral indices being by unity plus higher than those of protons.

Both types of particles, electrons and protons, produce turbulence cause by two beam instabilities (transit and bounced beams) which moves with the beam outside from the X-nullpoint.

These characteristics of energetic particles gained during their passage of a reconnecting current sheets can explain many puzzling incosistencies in the in-situ observations of the solar wind in the vicinity of the heliospheric current sheet [13] and during passage of interplanetary Coronal Mass Ejections [18].

The current model is concentrated on the parameters of accelerated particles in a single current sheet while observations often show that current sheets can be broken into a number of magnetic islands [14, 18]. The investigation of more complex models with magnetic islands will be done in the forthcoming paper.

[1] Speiser T W 1965 *Journal of Geophysics Research* **70** 4219–+
[2] Litvinenko Y E and Somov B V 1993 *Solar Physics* **146** 127–133
[3] Litvinenko Y E 1996 *Astrophysical Journal* **462** 997–+
[4] Zharkova V V and Gordovskyy M 2004 *Astrophysical Journal* **604** 884–891
[5] Zharkova V V and Gordovskyy M 2005 *Space Science Reviews* **121** 165–188
[6] Wood P and Neukirch T 2005 *Solar Physics* **226** 73–95
[7] Oreshina A V and Somov B V 2006 *Astronomical and Astrophysical Transactions* **25** 261–273
[8] Zharkova V V and Gordovskyy M 2005 *Monthly Notices of the Royal Astronomical Society* **356** 1107–1116
[9] Zharkova V V and Agapitov O V 2009 *Journal of Plasma Physics* **75** 159–+
[10] Birn J, Drake J F, Shay M A, Rogers B N, Denton R E, Hesse M, Kuznetsova M, Ma Z W, Bhattacharjee A, Otto A and Pritchett P L 2001 *Journal of Geophysics Research* **106** 3715–3720
[11] Tsiklauri D and Haruki T 2007 *Physics of Plasmas* **14** 2905–+ (*Preprint* `arXiv:0708.1699`)
[12] Siversky T V and Zharkova V V 2009 *Journal of Plasma Physics* **75** 619–+
[13] Zharkova V V and Khabarova O V 2012 *Astrophysical Journal* **752** 35
[14] Drake J F, Swisdak M, Che H and Shay M A 2006 *Nature* **443** 553–556
[15] Priest E and Forbes T 2000 *Magnetic Reconnection* (Magnetic Reconnection, by Eric Priest and Terry Forbes, pp. 612. ISBN 0521481791. Cambridge, UK: Cambridge University Press, June 2000.)
[16] Shay M A, Drake J F, Denton R E and Biskamp D 1998 *Journal of Geophysics Research* **103** 9165–9176
[17] Shay M A and Drake J F 1998 *Geophysics Research Letters* **25** 3759–3762
[18] Khabarova O, Zank G, Li G, le Roux J A, Webb G M, Dosch A, Malandraki O E and Zharkova V V 2015 *AAS/AGU Triennial Earth-Sun Summit* (*AAS/AGU Triennial Earth-Sun Summit* vol 1) p 20501